Combining Ring-Opening Metathesis Polymerization and Cyclic Ester Ring-Opening Polymerization To Form ABA Triblock Copolymers from 1,5-Cyclooctadiene and D,L-Lactide

Louis M. Pitet and Marc A. Hillmyer*

Department of Chemistry, 207 Pleasant St. SE, University of Minnesota, Minneapolis, Minnesota 55455-0431

Received February 17, 2009; Revised Manuscript Received March 18, 2009

ABSTRACT: ABA triblock copolymers were synthesized by combining ring-opening metathesis polymerization (ROMP) of 1,5-cyclooctadiene (COD) with ring-opening polymerization of D,L-lactide. Hydroxyl-functionalized telechelic polyCOD was prepared by taking advantage of chain transfer during ROMP of COD using the acyclic chain transfer agent *cis*-1,4-diacetoxy-2-butene. These hydroxy-terminated macroinitiators were used as initiators for the polymerization of lactide to form a series of triblock copolymers with compositions in the range $0.24 \leq f_{PLA} \leq 0.89$ and molecular weights ranging from 22 to 196 kg mol^{-1}. The ordered-state morphologies of the triblocks were determined using small-angle X-ray scattering; well-ordered microstructures were observed for several samples, in accordance with the predicted dependence of morphology on composition. The mechanical properties of these materials were also investigated by performing tensile measurements; the triblocks were considerably tougher than poly(D,L-lactide), most markedly in samples with low polyCOD midblock content.

Introduction

The recent development and commercialization of ring-opening metathesis polymerization (ROMP) catalysts exhibiting unprecedented thermal and functional group tolerance have enabled the ready preparation of a versatile array of polymeric materials[1−3] including both telechelic and hemitelechelic polymers that have functionality on either both or one chain terminus, respectively. Telechelics are an important class of polymeric material in adhesive technology and polyurethane chemistry and as precursors for the preparation of block copolymers.[4] Utilizing ROMP, end-functionalized macromolecular precursors for block copolymer synthesis may be prepared by (1) using functionalized metathesis catalysts,[5−7] (2) terminating a living ROMP reaction with an appropriately functionalized reagent (e.g., ethyl vinyl ether derivatives for Ru-based catalysts),[8−10] or (3) introducing a functionalized acyclic chain transfer agent (CTA) with a cyclic monomer.[11]

Linear block copolymers have been prepared from mechanistically incompatible monomers by combining ROMP of cyclic olefins with atom-transfer radical polymerization (ATRP),[9,10,12−15] reversible addition−fragmentation chain-transfer (RAFT) polymerization,[16] and anionic polymerization.[17] Likewise, hydroxyl-terminal polymers are effective initiators for the ring-opening polymerization (ROP) of cyclic esters to produce block polymers. Combining ROMP with ROP was described by Katayama and co-workers, in which the vinyl termini of hemitelechelic polynorbornene (PNB) were converted to hydroxyl groups that were subsequently used to initiate the ring-opening polymerization of ε-caprolactone, yielding diblock copolymers.[13]

In the face of rising oil prices and voluminous landfills, increasing scrutiny is falling on petroleum-based plastic commodities, which has shifted the limelight toward materials comprising, for example, polylactide (PLA). This polymer boasts a renewable feedstock, biocompatibility, and biodegradability and has proven suitable for a number of packaging and food containment applications.[18−20] Looming economic challenges and resource scarcity encourage the use of PLA in an increasing array of commodity products, an endeavor that requires specific tailoring of the mechanical properties.[20,21] Amorphous PLA homopolymer has a high tensile modulus but suffers low toughness, a deficiency that may be addressed by exploiting some fundamental characteristics of block copolymers.[22] As an example, soft components that are tethered in triblock copolymers with an ABA architecture may impart elasticity and/or toughness to brittle materials, as in the case of poly(styrene)-*b*-poly(butadiene)-*b*-poly(styrene) copolymers. Alternatively, triblocks may be introduced in two-component blends to manipulate the dispersion, as demonstrated in PLA blends with tougher materials such as polyethylene; block copolymers comprising the two components were introduced to improve the compatibilization.[23−26] The volume of literature exploring the synthesis and properties of PLA in the past decade[27,28] illustrates the growing importance of this environmentally friendly material.[29]

In this report, we describe the synthesis of symmetric ABA triblock copolymers containing PCOD midblocks and PLA end blocks with the aim of producing PLA samples with enhanced toughness. The synthesis requires a two-step process utilizing ROMP of COD by the second-generation Grubbs catalyst (**1**) in the presence of a chain transfer agent first, followed by ROP of D,L-lactide initiated by the terminal hydroxyl functionality in the PCOD precursor (Scheme 1). The morphological characteristics of these triblocks were examined using small-angle X-ray scattering and were compared with the theoretical phase behavior of linear triblock copolymers exhibiting narrow molecular weight distributions. The tensile properties of a series of triblocks with variable composition were examined and compared with those of the respective homopolymers.

Results and Discussion

Synthesis of Triblock Copolymers. Preparation of hydroxy telechelic PCOD has been reported previously using a variety of methods including via addition of an acyclic CTA during ROMP of COD.[30−38] For example, basic hydrolysis of acetoxy groups at the termini of either PCOD or PNB yields hydroxyl functional chains by using the appropriately substituted CTA.[33,35,39] This approach exhibits high conversions and well-controlled degree of polymerization and was thus chosen as the

* Corresponding author. E-mail: hillmyer@umn.edu.

10.1021/ma900368a CCC: $40.75
Published on Web 04/29/2009

Scheme 1. Synthesis of Triblock Copolymer LCL Using Ring-Opening Metathesis Polymerization of Cyclooctadiene Followed by Ring-Opening Polymerization of D,L-Lactide

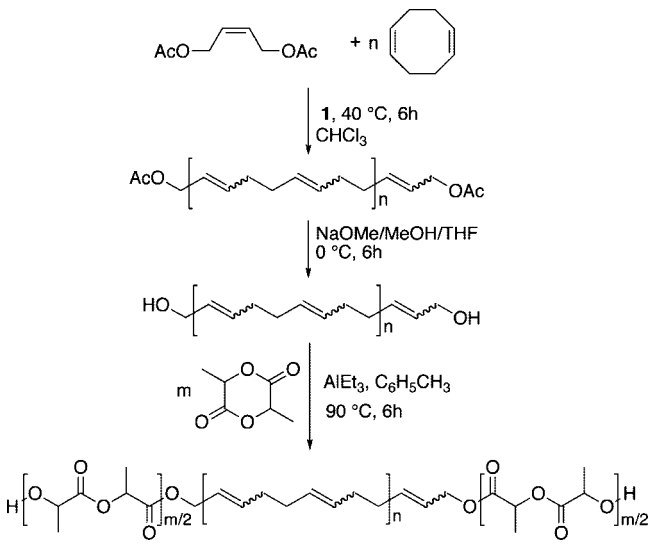

synthetic route for preparing the precursor macroinitiators leading to the triblock copolymers described in this study.

A single hydroxy telechelic PCOD sample was prepared. We employed low catalyst loadings ([COD]/[catalyst] = 15 000), and thus the ratio of [COD] to [CTA] determines the final molecular weight of the PCOD homopolymer according to eq 1

$$M_n = \frac{[\mathrm{COD}] m_{\mathrm{COD}} x_{\mathrm{COD}}}{[\mathrm{CTA}]} \quad (1)$$

where m_{COD} is the molar mass of the monomer[40] and x_{COD} is the fractional conversion of COD, which was essentially quantitative ($\approx$1) based on ^{1}H NMR spectroscopy of the reaction mixtures. The functional CTA we used was *cis*-1,4-diacetoxy-2-butene (DAB). Additionally, commercially available and freshly distilled COD monomer contains the isomer vinylcyclohexene (VCH), which acts as adventitious CTA.[41] We employed a [COD] to [DAB] ratio of 150 making the DAB concentration equal to 0.67 mol %, while ^{1}H NMR spectroscopy showed 0.16 mol % of VCH in the freshly distilled monomer. The combined concentrations of CTAs applied to eq 1 gives a theoretical M_n equal to 13.0 kg mol^{-1}. We identified both acetoxy and vinyl end groups in the ^{1}H NMR spectrum of AcO−PCOD−OAc derived from the DAB and VCH, respectively. The calculated M_n of this precursor was 16.4 kg mol^{-1}, which suggests incomplete incorporation of CTA in the polymer. We calculated the molar ratio of [DAB] to [VCH] before polymerization of 4.2 compared to a value of 3.5 from the relative signals in the ^{1}H NMR spectrum of the polymer, which suggests that VCH reacts more readily than does DAB. Using these quantities, the average number of hydroxyl functional end groups per polymer chain (F_n) is calculated as F_n = 1.5. Therefore, there are both monofunctional and nonfunctional chains that bear vinyl and/or cyclohexenyl moieties resulting from rapid secondary metathesis reactions throughout polymerization, although difunctional chains arguably constitute the majority of molecules. It is possible to attain F_n values approaching 2 with extensive purification of COD feedstock.[41] However, we forwent the procedure, being motivated by the potential for practical applications using readily available starting materials.

Deprotection of the acetoxy termini using a solution of NaOMe in methanol/THF gave hydroxy telechelic PCOD (HO−PCOD−OH). Parts a and b of Figure 1 show the size-exclusion chromatography (SEC) chromatograms for the telechelic PCOD samples before and after hydrolysis, respectively. The overlap between the two traces demonstrates the preservation of the overall characteristics. The M_n determined by ^{1}H NMR spectroscopy after hydrolysis was 15.6 kg mol^{-1}, in agreement with the precursor molecular weight. The PDI values for the telechelic PCOD samples before and after hydrolysis were 1.80 and 1.72, respectively, as measured by SEC relative to polystyrene standards. There is a broad peak eluting between 23 and 25 mL in both samples presumably associated with a low level of low molecular weight cyclic oligomers.

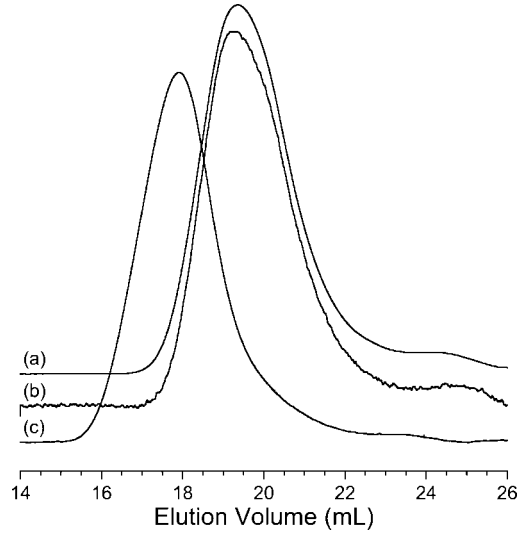

Figure 1. SEC chromatograms: (a) AcO−PCOD−OAc, (b) HO−PCOD−OH, (c) LCL (35−16−35) illustrating the incorporation of D,L-lactide into the polymer chains. The data in part c are consistent with the absence of significant HO−PCOD−OH.

Poly(D,L-lactide)−poly(cyclooctadiene)−poly(D,L-lactide) (LCL) triblock copolymers were prepared by growing poly(D,L-lactide) from the telechelic PCOD precursor (Scheme 1). Triethyl aluminum was used to prepare macromolecular aluminum alkoxide species that effect initiation of ROP of various lactones and lactide.[42−44] The SEC chromatogram for sample LCL (35−16−35) (the numbers correspond to the number average molecular weights of each block in kg mol^{-1}) is shown as a representative example in Figure 1c. Distinct peaks associated with unreacted PCOD were absent in all samples. The molecular characteristics of the LCL copolymers are summarized in Table 1.

Figure 2 includes the region of the ^{1}H NMR spectrum corresponding to the end-group methylene protons for the protected PCOD associated with AcO−PCOD−OAc. After hydrolysis of the acetate groups, the end-group methylene protons shift upfield. Complete hydrolysis is indicated by disappearance of signals at δ = 4.1 ppm (Figure 2). The ring-opening polymerization of D,L-lactide using the hydroxyl groups as initiating moieties leads to a shift of the signal associated with the same protons to δ = 4.50−4.70 ppm, as exemplified for LCL (13−16−13) in Figure 2. An additional signal associated with the methine protons on the lactide chain ends is present at δ = 4.31−4.41 ppm. The full spectrum for LCL (13−16−13) is also shown in Figure 2. The integration ratio of the midmethylene and end-group methine protons is 2.07 (theoretically the ratio should be 2), consistent with the absence of adventitious initiator for the lactide polymerization, the absence of significant PLA homopolymer, and a high initiation efficiency.

The ratio of cis to trans configuration for the double bonds in the precursors and triblocks is equal to 0.19 (84% trans),

Table 1. Molecular Characteristics of Telechelic PCOD Precursors and LCL Triblock Copolymers

sample ID[a]	f_{PLA}[b]	M_n[c]/kg mol^{-1}	PDI[d]	T_m/°C	ΔH_m[e]/J g^{-1}	X_{PCOD}[f]/%	D[g]/nm 150 °C	D[g]/nm 35 °C
AcO−C−OAc	0.00	16.4	1.80					
HO−C−OH	0.00	15.6	1.72	26	69	80		
LCL (3.4−16−3.4)	0.24	22.5	1.55	22	40	68	32.4	32.0
LCL (5.6−16−5.6)	0.34	26.8	1.50	22	27	53	33.2	34.5
LCL (8.6−16−8.6)	0.44	32.9	1.60	24	20	49	38.5	38.5
LCL (13−16−13)	0.54	41.0	1.53	23	15	47	44.6	44.7
LCL (20−16−20)	0.65	56.4	1.70	21	6.6	28	49.1	53.9
LCL (35−16−35)	0.76	85.7	1.87	21	3.4	23	36.5	37.3
LCL (90−16−90)	0.89	195	1.40	19	1.3	19	43.6	44.3

[a] Sample ID corresponds to molecular weights of the respective blocks calculated by ^{1}H NMR spectroscopy. [b] Volume fraction of PLA was calculated using the densities for the polymers at 25 °C; $\rho_{PLA} = 1.25$ g cm^{-3} and $\rho_{PCOD} = 0.89$ g cm^{-3} from refs 45 and 46, respectively. [c] Determined from integration of the corresponding repeat unit protons in ^{1}H NMR spectra relative to end-group signals of the precursor macromolecular initiator. [d] Determined from SEC with $CHCl_3$ as the eluent at 35 °C, relative to narrow distribution polystyrene standards. [e] Determined from integration of the melting endotherm on the second heat during DSC analysis. [f] Calculated using $\Delta H_m^0 = 85.2$ J g^{-1} for completely linear *all-trans*-poly(1,4-butadiene)[47] and normalized to the midblock using weight fractions (w) calculated from ^{1}H NMR spectroscopy [$X_{PCOD} = \Delta H_m/(\Delta H_m^0 w_{PCOD})$]. [g] Principle domain spacing determined by SAXS using $D^* = 2\pi/q^*$.

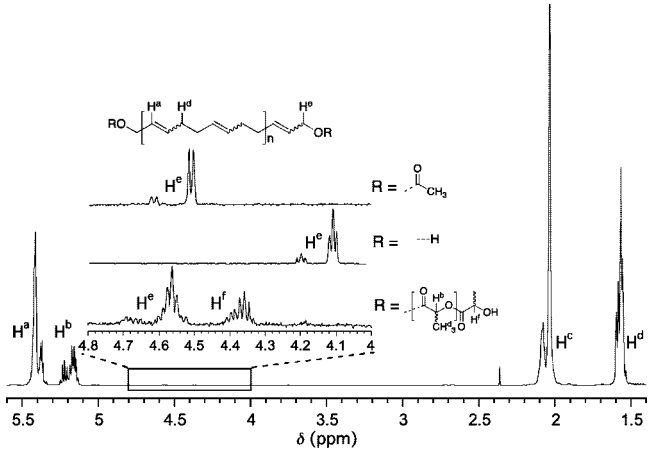

Figure 2. ^{1}H NMR spectra for telechelic PCOD homopolymer precursors before (AcO−PCOD−OAc, top) and after (HO−PCOD−OH, middle) hydrolysis with signals corresponding to the cis and trans methylene end-group protons. The spectrum for sample LCL (13−16−13) is shown in full with the bottom inset region corresponding to the cis and trans midmethylene protons and the end-group methine protons on the PLA chains, H^f.

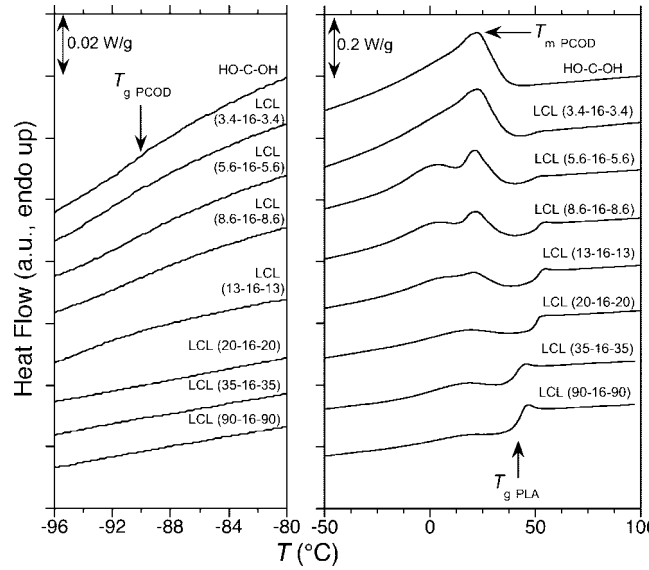

Figure 3. DSC traces for the LCL triblocks. The temperatures associated with characteristic transitions are indicated. Traces represent the second heat after annealing at 160 °C with a heating rate of 10 °C min^{-1}.

which is characteristic of ROMP polymerizations with extensive intermolecular chain transfer.

Thermal Analysis. Samples in Table 1 were analyzed by DSC by first heating to 160 °C, annealing for 5 min at 160 °C, cooling to −100 °C at 10 °C min^{-1} and reheating to 120 °C at 10 °C min^{-1}. The data for the final reheating is shown in Figure 3. Consistent with microphase separation, glass transitions signatures around 47 °C for the PLA blocks and −95 °C for the PCOD blocks were observed for all but highly compositionally asymmetric LCL samples. High trans PCOD is semicrystalline and the melting temperature (T_m) of the PCOD blocks was observed between 20 and 25 °C. The breadth of this transition is likely due to a distribution of crystallite sizes. The T_m values and percent crystallinities (X_{PCOD}) are provided in Table 1.

A monotonic decrease in both crystallinity and T_m with increasing PLA content was observed. This could arise from the topological restriction imposed by the glassy PLA forcing confined crystallization in samples with majority PLA. Also, bimodality in the PCOD melting endotherm is clearly evident in samples LCL (13−16−13), LCL (8.6−16−8.6), and LCL (5.6−16−5.6). There are two possible factors that contribute to this behavior. The relatively wide breadth of the peaks likely results from a broad distribution of trans-sequence lengths in the PCOD block.[48] Additionally, the large number of microdomains in the phase-separated material causes crystallization during cooling by different mechanisms (i.e., hetero- vs homogeneous nucleation).[49,50] Crystallites of two distinct size distributions likely exist, which manifests as multiple melting endotherms. This hypothesis is supported by the apparent absence of distinct endotherms in sample LCL (3.4−16−3.4), in which the crystalline PCOD occupies a continuous domain.

Morphological Characteristics. Diblock copolymers can self-assemble into four classical equilibrium structures [lamellar (L), bicontinuous gyroid (G), hexagonally packed cylinders (C), and spheres on a body centered cubic lattice (S)], dependent on the composition and the degree of segregation, which is the product of the degree of polymerization, N, and the relative incompatibility of the species represented by the Flory−Huggins interaction parameter, χ.[51−56] These structures may be identified by small-angle X-ray scattering.

One-dimensional small-angle X-ray scattering (SAXS) patterns at both 150 and 35 °C for the triblock copolymers are illustrated in parts a and b of Figure 4, respectively. The plots are presented as scattered intensity with respect to the scattering momentum vector $q = 4\pi/\lambda(\sin\theta/2)$, where θ is the scattering angle and λ is the wavelength of incident radiation. All LCL samples exhibited microphase separation as evidenced by a sharp principal peak (q^*) at low scattering angle (Figure 4a). The

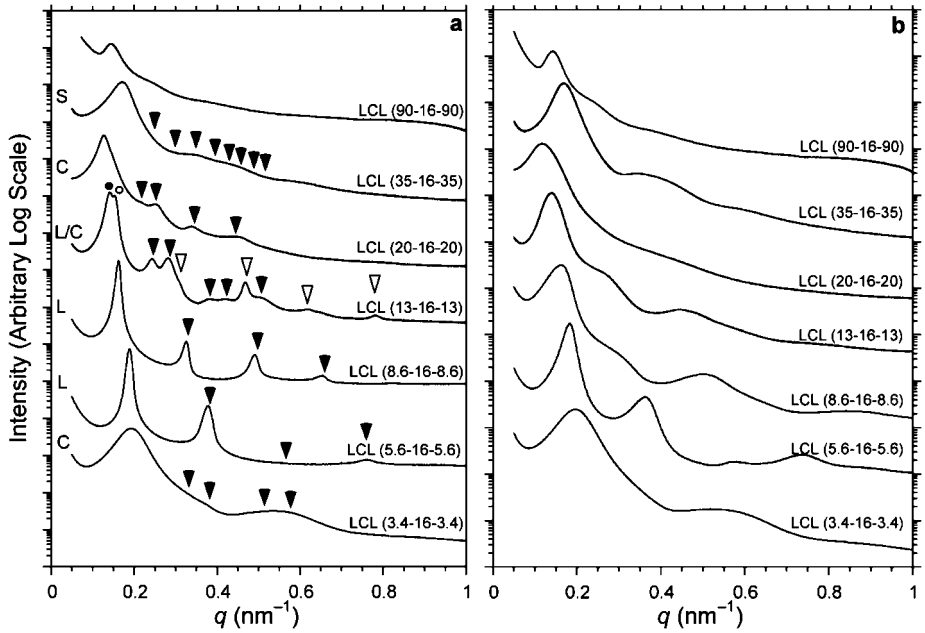

Figure 4. One-dimensional SAXS profiles for representative LCL triblock copolymers measured at (a) 150 °C after 5 min annealing times with the arrows indicating the predicted peak positions for the indicated morphologies (L = lamellae; C = cylinders; G = gyroid; S = spheres) and (b) at 35 °C after cooling from 150 °C. Sample LCL (13−16−13) exhibits coexisting morphologies with empty arrows indicating L and full arrows indicating C.

predicted peak positions are indicated by arrows and correspond to the theoretically expected morphology at the specific volume fractions taking into consideration the architecture and the somewhat polydisperse nature of the samples.[57] The principal domain spacing ($D^* = 2\pi/q^*$) values (Table 1) are consistent with variation in molecular weight, temperature, and morphological transitions.[58]

For the majority of samples, the principal spacing measured at 35 °C is larger than at 150 °C, consistent with increasing χ with decreasing temperature.[59] The lowest molecular weight sample LCL (3.4−16−3.4) exhibits the smallest domain spacing at 32.4 nm (150 °C) and a SAXS profile consistent with hexagonally packed cylinders of PLA in a PCOD matrix. Both samples LCL (5.6−16−5.6) and LCL (8.6−16−8.6) have SAXS profiles consistent with a lamellar morphology. Sample LCL (13−16−13) appears to have coexisting lamellar and cylindrical morphologies at 150 °C. This is consistent with calculations that predict relatively large windows of coexisting C and L phases at large segregation strengths and when the minority component (PCOD) is the more polydisperse block.[60] The SAXS profile for sample LCL (20−16−20) is consistent with a matrix of PLA with cylinders of PCOD, while that of both LCL (35−16−35) and LCL (90−16−90) are consistent with being dispersions of PCOD spheres in a PLA matrix.

The *D*-spacing increases monotonically with M_n until the apparent transition from cylinders of PCOD in a PLA matrix [LCL (20−16−20)] to spheres of PCOD in a PLA matrix [LCL (35−16−35)]. The decrease in D^* with increasing M_n going from LCL (20−16−20) to LCL (35−16−35) is consistent with the established dependence of domain spacing on morphology;[58] the decrease in D^* associated with traversing the C → S phase boundary apparently outweighs the opposing increase in D^* with increasing molecular weight.

The morphologies of LCL (35−16−35) and LCL (90−16−90) are believed to be an array of PCOD spheres embedded in a PLA matrix despite the relatively ill-resolved high-order reflections in Figure 4 for these samples. LCL (90−16−90) exhibits a sharp primary peak at $q^* = 0.149$ ($D^* = 42$ nm) with several additional broad peaks at higher *q*-values. This is typical of a disordered array of micelles in which the minority component is dispersed in a "solution" of the majority component. We analyzed the scattering for LCL (90−16−90) using the spherical form factor shown in eq 2:

$$P(q) = \left(\frac{3}{(qR)^3}\right)^2(\sin qR - qR\cos qR)^2 \qquad (2)$$

We initially determined the cylinder radius (R_c) for samples LCL (20−16−20) (R_c = 17.6 nm) and LCL (13−16−13) (R_c = 18.3 nm) and assumed that this value would be approximately equal to the radii of the spheres in samples LCL (35−16−35) and LCL (90−16−90). We calculated R_c for these two cylindrical samples using D^* from SAXS, the volume fraction of PCOD (f_c), and the following expression: $R_c = (2f_cD^{*2}/\sqrt{3}\pi)^{1/2}$. The simulated form factor scattering corresponding to eq 2 with R = 16 nm is provided with the actual scattering pattern obtained for sample LCL (90−16−90) in Figure 5. This value (R = 16 nm) provided the best match to the experimental pattern, suggesting that the sphere radii are slightly smaller than the cylinder radii. This observation is consistent with a larger interfacial curvature and thus increased stretching experienced by the minority component in spheres compared to cylinders.[58] The minima in the fit correspond reasonably well with several peak minima in the actual scattering, in agreement with the implicated morphology. Sample LCL (35−16−35) also exhibited form-factor scattering consistent with the indicated block size and proposed morphology.

To corroborate the SAXS data, transmission electron microscopy (TEM) images for samples LCL (8.6−16−8.6) and LCL (90−16−90) were acquired (Figure 6). LCL (8.6−16−8.6) was aligned using a channel-die as described previously,[61] and microtoming was performed perpendicular to the flow direction. The lamellar spacing from TEM (34 nm) agrees reasonably well with D^* from the SAXS data (38.5 nm). Sample LCL (90−16−90) appears to consist of a disorganized array of spherical PCOD domains (dark) surrounded by the unstained PLA (light). The sphere diameter is approximately 30 nm, agreeing reasonably well with the value obtained from form factor modeling in the SAXS (see Figure 5 and eq 2).

Mechanical Properties. PLA property modification is the focus of many research efforts, the more recent of which have

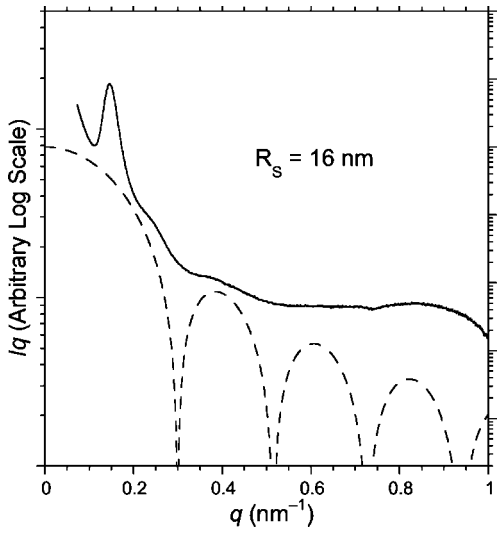

Figure 5. Form factor scattering simulation (---) correlated with actual scattering data (—) for sample LCL (90−16−90). The form-factor fit utilizes a 16 nm sphere radius based on the actual domain spacing from samples adopting the cylindrical morphology.

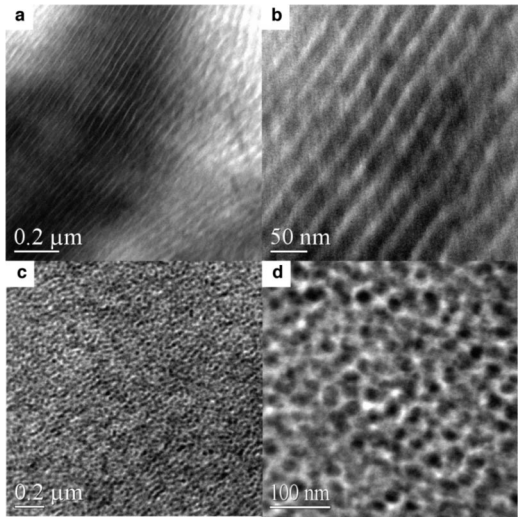

Figure 6. TEM images (stained with OsO_4) at different magnifications for sample LCL (8.6−16−8.6) (a, b) showing lamellae of PCOD (dark) and PLA (light) and LCL (90−16−90) (c, d) showing a disordered array of PCOD (dark) spheres in a matrix of PLA (light).

Table 2. Mechanical Properties of Triblock LCL Copolymers[67]

sample ID	modulus/MPa	σ_b/MPa	ε_b/%
LCL (3.4−16−3.4)	5.6 ± 2.0	0.9 ± 0.2	43 ± 7
LCL (5.6−16−5.6)	50.7 ± 5.2	2.7 ± 0.3	18 ± 6
LCL (8.6−16−8.6)	89 ± 30	6.8 ± 0.5	36 ± 5
LCL (13−16−13)	308 ± 48	11 ± 2	33 ± 27
LCL (20−16−20)	448 ± 170	17 ± 3	32 ± 41
LCL (35−16−35)	864 ± 224	20 ± 4	180 ± 170
LCL (90−16−90)	1270 ± 380	33 ± 1	42 ± 17

been thoroughly reviewed.[22] We have used a soft ($T_g = -100$ °C; $T_m = 20$ °C), semicrystalline component tethered on either end by PLA to improve the toughness while attempting to maintain a high yield strength and modulus compared to PLA homopolymer. This method has proven successful, as exemplified in the case of poly(cyclohexylethylene)-*b*-polyethylene-*b*-poly(cyclohexylethylene) in which a semicrystalline midblock is flanked by glassy end blocks.[62,63]

The LCL tensile properties are summarized in Table 2. In each experiment, dogbones were prepared by melt pressing at 160 °C and 1000 psi followed by rapid cooling to 25 °C (ca.

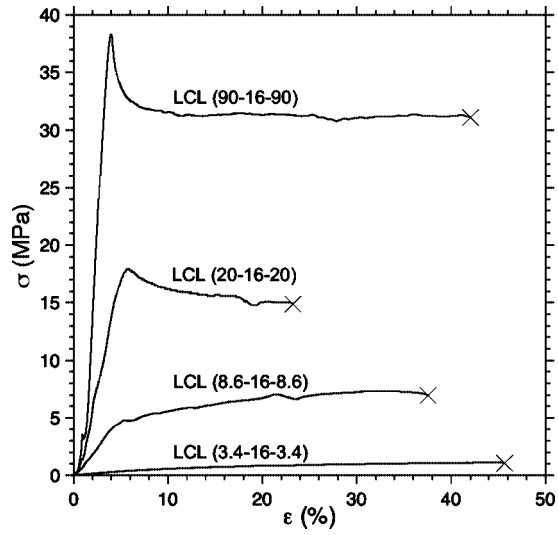

Figure 7. Tensile measurements for selected LCL triblock copolymers presented as engineering stress ($\sigma = F/A$) as a function of engineering strain percent ($\varepsilon = 100 \times \Delta L/L_0$), showing the progression of tensile modulus, yield strength, and tensile strength. The fracture point is represented by the symbol ×.

30 °C min^{-1}) and then uniaxial extension was applied at a rate of 2 mm min^{-1} until the samples fractured. A representative set of tensile results are illustrated in Figure 7 for samples LCL (3.4−16−3.4), LCL (8.6−16−8.6), LCL (20−16−20), and LCL (90−16−90). The tensile modulus of amorphous PLA ranges from 2 to 4 GPa, depending on processing conditions and molecular weight.[64,65] For amorphous PLA having molecular weights between 50 and 200 kg mol^{-1}, the tensile strength was measured in the range of 40−50 MPa. However, typical elongation when fracture occurs ranges from approximately 3 to 10% for amorphous PLA homopolymer.[21,27,66]

The modulus, tensile strength, and yield strength all increase monotonically with increasing molecular weight of the LCL samples. This can be attributed to increasing PLA content and molecular weight. Interestingly, neither the yield strain nor strain at break exhibit noticeable dependence on composition or molecular weight.[68] The samples with the highest PLA content exhibit the largest modulus, tensile strength, and yield strength values with ultimate elongations an order of magnitude greater than typical values for PLA homopolymer. Most notably, the sample LCL (90−16−90) has a modulus of 1.3 GPa, an average elongation of 42%, a yield strength of 38 MPa, and tensile strength of 33 MPa. These values are consistent with significant toughness in a sample of PLA containing less than 10 wt % of a rubbery component.

Experimental Details

Materials. 1,5-cyclooctadiene was purchased from Aldrich (99%) and was distilled over CaH_2 prior to use. Grubbs second-generation catalyst was a gift from Materia and was used as received. D,L-Lactide (99.5%) purchased from Purac was recrystallized twice from ethyl acetate and stored under a N_2 atmosphere. Triethyl aluminum was purchased as a 1.0 M solution in heptane from Aldrich. The chain transfer agent *cis*-2-butene-1,4-diol diacetate (>95%) obtained from TCI America was vacuum distilled. Chloroform from Mallinckrodt was thoroughly degassed prior to use with a N_2 purge. Toluene from Mallinckrodt was passed over an alumina column prior to use. Methanol was also purchased from Mallinckrodt and was used as received. Sodium methoxide and hydrochloric acid were from Aldrich and were used as received.

Characterization. ^{1}H NMR spectroscopy was performed on a Varian Inova 500 instrument operating at 500 MHz. Solutions were prepared in $CDCl_3$ (Cambridge Isotope Laboratories) at ap-

proximately 15 mg/mL. All spectra were obtained at 20 °C after 64 transients using a relaxation delay of 5 s with chemical shifts reported as δ (ppm) relative to the ^{1}H signals from hydrogenous solvent (7.27 ppm for $CHCl_3$).

Size-exclusion chromatography was used to evaluate the molecular weight evolution and polydispersity index in the triblock copolymers. Samples were prepared at concentrations near 1 mg/mL in $CHCl_3$. The instrument operates at 35 °C using three Plgel 5 μm Mixed-C columns in series with molecular weight range 400−400 000 g mol^{-1}. The columns are housed in a Hewlett-Packard (Agilent Technologies) 1100 series liquid chromatograph equipped with a Hewlett-Packard 1047A refractive index detector. PDIs are reported with respect to polystyrene standards obtained from Polymer Laboratories.

Small-angle X-ray scattering experiments were performed at the Advanced Photon Source (APS) at Argonne National Laboratories at Sector 5-ID-D beamline. The beamline is maintained by the Dow−Northwestern−Dupont Collaborative Access Team (DND-CAT). The source produces X-rays with a wavelength of 0.84 Å. The sample to detector distance was 5.65 m and the detector radius is 81 mm. Scattering intensity was monitored by a Mar 165 mm diameter CCD detector with a resolution of 2048 × 2048. The two-dimensional scattering patterns were azimuthally integrated to afford one-dimensional profiles presented as spatial frequency (q) versus scattered intensity.

Differential scanning calorimetric measurements were obtained using a DSC Q-1000 calorimeter from TA Instruments that was calibrated with an indium standard. Samples were loaded into hermetically sealed aluminum pans prior to analysis. The thermal history of the samples were all erased by heating the samples to 160 °C and isothermally annealing for 5 min. The samples were then cooled at 10 °C min^{-1} to −110 °C followed by a second heating cycle to 160 °C at a rate of 10 °C min^{-1}, all under a nitrogen purge. Melting enthalpies were evaluated by integration of the melting endotherm using TA Universal Analysis software.

Mechanical properties were obtained using small dog-bone samples of the polymers that were cut from a mold after pressing at 160 °C under 1000 psi. The samples had the approximate dimensions of 0.5 mm (T) × 3 mm (W) × 15 mm (L). The tensile measurements were performed on a Rheometrics Scientific MiniMat instrument. Samples were extended lengthwise uniaxially at 2.0 mm min^{-1}.

Ultrathin sections (ca. 70 nm) of the polymer films were cut using a Reichert UltraCut S Ultramicrotome with a Model FC-S addition, allowing microtoming at −120 °C. The thin sections were mounted on 400 mesh copper grids and stained with OsO_4 vapor for 15 min from a 4% aqueous solution. TEM was performed on a JEOL JEM-1210 microscope operating at 120 keV. Images were captured with a Gatan Multiscan CCD camera.

Synthesis. The synthesis of hydroxy telechelic poly(cyclooctadiene) was adapted from a literature procedure.[33,35] The precursor HTPCOD used for all triblock copolymers was prepared as described. A 150 mL portion of $CHCl_3$ was added to a flame-dried 500 mL round-bottom single-neck flask and was thoroughly purged with N_2 gas. Then 0.42 mL (0.46 g, 2.6 mmol) of the CTA was added using a gastight syringe. Grubbs second generation catalyst (22 g, 26 mmol) was added as a solution in 1.0 mL of $CHCl_3$ using a gastight syringe. The mixture was immersed in a oil-bath at 40 °C with rapid stirring. COD (50.0 mL, 43 g, 398 mmol) was added dropwise using a glass syringe over 1 h. The polymerization mixture was rapidly stirred for 8 h at 40 °C. The reaction was simultaneously quenched with and precipitated into 1 L of MeOH containing 15 mL of 1 M HCl (aq). The polymer was isolated by filtration and dried further under reduced pressure for 24 h. ^{1}H NMR ($CDCl_3$): δ 5.40−5.45 (m, (*E*)-C*H*═C*H*CH$_2$−, backbone), 5.35−5.40 (m, (*Z*)-C*H*═C*H*CH$_2$−, backbone), 4.62 (d, (*E*)-CH═CHC*H*$_2$OAc), 4.51 (d, (*Z*)-CH═CHC*H*$_2$OAc), 2.06−2.11 (m, (*Z*)-CH═CHC*H*$_2$− backbone), 2.01−2.06 (m, (*E*)-CH═CHC*H*$_2$− backbone).

The entire yield (39.6 g, 92%) was dissolved in 500 mL of THF at 0 °C. Twenty-five milliliters of a 0.7 M solution of NaOMe in MeOH (0.94 g, 17.5 mmol NaOMe) was added dropwise over 1 h. The mixture was allowed to stir at 0 °C for 5 h, at which point the polymer was precipitated into 2 L of cold MeOH containing 15 mL of 1 M HCl (aq). The polymer was isolated by filtration and vacuum-dried at room temperature for 24 h, yielding 37.9 g (88.1%). ^{1}H NMR ($CDCl_3$): δ 5.40−5.45 (m, (*E*)-C*H*═C*H*CH$_2$− backbone), 5.35−5.40 (m, (*Z*)-C*H*═C*H*CH$_2$−, backbone), 4.18 (t, (*Z*)-CH═CHC*H*$_2$OH) 4.11 (t, (*E*)-CH═CHC*H*$_2$OH), 2.06−2.11 (m, (*Z*)-CH═CHC*H*$_2$− backbone), 2.01−2.06 (m, (*E*)-CH═CHC*H*$_2$− backbone).

The synthesis of the entry in Table 1 labeled LCL (8.6−16−8.6) is described here. Variable compositions were achieved by manipulating the relative amounts of D,L-lactide, Al(Et)$_3$, and toluene added to the reaction mixture. The precursor HO−C−OH (2.0 g, 20.5 kg mol^{-1}, 9.75 × 10^{-2} mmol OH) was placed in a 48 mL pressure vessel with a Teflon screw-cap and a Teflon-coated stirbar. The flask was placed in a glovebox with a nitrogen atmosphere where 17 mL of toluene and 97 μL of a 1 M solution of Al(Et)$_3$ in heptane were added via syringe. The molar ratio of −OH to Al was kept constant at 3:1. This reaction was stirred for 6 h at room temperature to functionalize the aluminum catalyst, creating the aluminum alkoxide species used to initiate ring-opening polymerization of the cyclic ester. D,L-lactide (2.50 g, 17.3 mmol) was placed in the vessel before sealing and removing from the glovebox. The vessel was then immersed into an oil bath at 90 °C. The polymerization solution was allowed to react for 8 h before quenching with 2 mL of 1 M HCl (aq). The final solution was precipitated into 150 mL of MeOH with rapid stirring and the polymer was isolated by filtration. After drying at room temperature for 24 h at reduced pressure (ca. 20 mTorr), the yield was 79%. ^{1}H NMR ($CDCl_3$): δ 5.40−5.45 (m, (*E*)-C*H*═C*H*CH$_2$− backbone), 5.35−5.40 (m, (*Z*)-C*H*═C*H*CH$_2$−), 5.13−5.27 (m, −C(O)C*H*(CH$_3$)O− backbone), 4.62−4.70 (m, (*Z*)-CH═CHC*H*$_2$OC(O)C(CH$_3$)−), 4.52−4.62 (m, (*E*)-CH═CHC*H*$_2$OC(O)C(CH$_3$)−), 4.33−4.42 (m, C(O)C*H*(CH$_3$)OH), 2.06−2.11 (m, (*Z*)-CH═CHC*H*$_2$− backbone), 2.01−2.06 (m, (*E*)-CH═CHC*H*$_2$− backbone), 1.52−1.61 (m, −C(O)CH(C*H*$_3$)O− backbone).

Conclusions

We have demonstrated a straightforward two-step synthesis of linear triblock copolymers by combining ROMP of COD with ROP of D,L-lactide. The PCOD midblock was prepared by utilizing a chain transfer agent in the ROMP of COD with a commercial Ru catalyst ultimately yielding hydroxy-terminated PCOD. The hydroxy functionality was employed to initiate ROP of D,L-lactide to give triblock copolymers with molecular characteristics dictated by the feedstock composition. Microphase separation was evidenced by well-defined peaks in the one-dimensional SAXS profiles. By tethering a soft midblock component with characteristically brittle PLA, tough and strong materials were realized. Tensile measurements showed impressive elongation at break for several samples with only small volume fractions of PCOD while maintaining a relatively high tensile modulus attributed to high PLA content.

Acknowledgment. This work was supported by the National Science Foundation (DMR-0605880). Parts of this work were carried out in the University of Minnesota I.T. Characterization Facility, which receives partial support from NSF through the NNIN program. SAXS data were acquired at the DuPont−Northwestern−Dow Collaborative Access Team (DND-CAT) located at Sector 5 of the Advanced Photon Source (APS). DND-CAT is supported by E. I. Dupont de Nemours and Co., The Dow Chemical Co., and the State of Illinois. Use of the APS was supported by the U.S. Department of Energy, Office of Science, Office of Basic Energy Sciences, under Contract No. DE-AC02-06CH11357. The authors would like to acknowledge Liang Chen for help with TEM and many helpful discussions. We also thank Dr. Nathaniel Lynd for helpful discussions and Prof. Mahesh Mahanthappa for preliminary synthetic trials.

References and Notes

(1) Bielawski, C. W.; Grubbs, R. H. *Prog. Polym. Sci.* **2007**, *32*, 1–29.
(2) Bielawski, C. W.; Grubbs, R. H. *Angew. Chem., Int. Ed.* **2000**, *39*, 2903–2906.
(3) Trnka, T. M.; Grubbs, R. H. *Acc. Chem. Res.* **2001**, *34*, 18–29.
(4) Goethals, E. J. *Telechelic Polymers: Synthesis and Applications* CRC Press: Boca Raton, FL, 1989.
(5) Bielawski, C. W.; Louie, J.; Grubbs, R. H. *J. Am. Chem. Soc.* **2000**, *122*, 12872–12873.
(6) Burtscher, D.; Saf, R.; Slugovc, C. *J. Polym. Sci., Part A: Polym. Chem.* **2006**, *44*, 6136–6145.
(7) Katayama, H.; Urushima, H.; Ozawa, F. *J. Organomet. Chem.* **2000**, *606*, 16–25.
(8) Chen, B.; Metera, K.; Sleiman, H. F. *Macromolecules* **2005**, *38*, 1084–1090.
(9) Matson, J. B.; Grubbs, R. H. *Macromolecules* **2008**, *41*, 5626–5631.
(10) Li, M.-H.; Keller, P.; Albouy, P.-A. *Macromolecules* **2003**, *36*, 2284–2292.
(11) Bielawski, C. W.; Hillmyer, M. A. In *Handbook of Metathesis*; Grubbs, R. H., Ed.; Wiley-VCH: Weinham, Germany, 2003; Vol. 3, pp 255−282.
(12) Coca, S.; Paik, H.-J.; Matyjaszewski, K. *Macromolecules* **1997**, *30*, 6513–6516.
(13) Katayama, H.; Fukuse, Y.; Nobuto, Y.; Akamatsu, K.; Ozawa, F. *Macromolecules* **2003**, *36*, 7020–7026.
(14) Bielawski, C. W.; Morita, T.; Grubbs, R. H. *Macromolecules* **2000**, *33*, 678–680.
(15) Katayama, H.; Yonezawa, F.; Nagao, M.; Ozawa, F. *Macromolecules* **2002**, *35*, 1133–1136.
(16) Mahanthappa, M. K.; Bates, F. S.; Hillmyer, M. A. *Macromolecules* **2005**, *38*, 7890–7894.
(17) Myers, S. B.; Register, R. A. *Macromolecules* **2008**, *41*, 5283–5288.
(18) Drumright, R. E.; Gruber, P. R.; Henton, D. E. *Adv. Mater.* **2000**, *12*, 1841–1846.
(19) Gruber, P. R.; O'Brien, M. *Biopolymers* **2002**, *4*, 235–250.
(20) Vink, E. T. H.; Rabago, R.; Glassner, D. A.; Springs, B.; O'Connor, R. P.; Kolstad, J.; Gruber, P. R. *Macromol. Biosci.* **2004**, *4*, 551–564.
(21) Auras, R.; Harte, B.; Selke, S. *Macromol. Biosci.* **2004**, *4*, 835–864.
(22) Anderson, K. S.; Schreck, K. M.; Hillmyer, M. A. *Polym. Rev.* **2008**, *48*, 85–108.
(23) Schreck, K. M.; Hillmyer, M. A. *J. Biotechnol.* **2007**, *132*, 287–295.
(24) Anderson, K. S.; Hillmyer, M. A. *Polymer* **2004**, *45*, 8809–8823.
(25) Anderson, K. S.; Lim, S. H.; Hillmyer, M. A. *J. Appl. Polym. Sci.* **2003**, *89*, 3757–3768.
(26) Wang, Y.; Hillmyer, M. A. *J. Polym. Sci., Part A: Polym. Chem.* **2001**, *39*, 2755–2766.
(27) Garlotta, D. *J. Polym. Environ.* **2002**, *9*, 63–84.
(28) Williams, C. K.; Hillmyer, M. A. *Polym. Rev.* **2008**, *48*, 1–10.
(29) Gross, R. A.; Kalra, B. *Science* **2002**, *297*, 803–807.
(30) Chung, T. C.; Chasmawala, M. *Macromolecules* **1992**, *25*, 5137–5144.
(31) Hillmyer, M. A.; Grubbs, R. H. *Macromolecules* **1993**, *26*, 872–874.
(32) Hillmyer, M. A.; Grubbs, R. H. *Macromolecules* **1995**, *28*, 8662–8667.
(33) Hillmyer, M. A.; Nguyen, S. T.; Grubbs, R. H. *Macromolecules* **1997**, *30*, 718–721.
(34) Morita, T.; Maughon, B. R.; Grubbs, R. H. *Polym. Prepr.* **1998**, *39*, 226–227.
(35) Bielawski, C. W.; Scherman, O. A.; Grubbs, R. H. *Polymer* **2001**, *42*, 4939–4945.
(36) Fraser, C.; Hillmyer, M. A.; Gutierrez, E.; Grubbs, R. H. *Macromolecules* **1995**, *28*, 7256–7261.
(37) Hilf, S.; Berger-Nicoletti, E.; Grubbs, R. H.; Kilbinger, A. F. M. *Ang. Chem. Int. Ed.* **2006**, *45*, 8045–8048.
(38) Hilf, S.; Grubbs, R. H.; Kilbinger, A. F. M. *Macromolecules* **2008**, *41*, 6006–6011.
(39) Bielawski, C. W.; Benitez, D.; Morita, T.; Grubbs, R. H. *Macromolecules* **2001**, *34*, 8610–8618.
(40) The contribution of the mass of the CTA to the overall molecular weight is considered negligible in calculating theoretical M_n as it constitutes approximately 1.3 wt % of the PCOD.
(41) Ji, S.; Hoye, T. R.; Macosko, C. W. *Macromolecules* **2004**, *37*, 5485–5489.
(42) Dubois, Ph.; Jerome, R.; Teyssie, P. *Makromol. Chem., Macromol. Symp.* **1991**, *42/43*, 103–116.
(43) Jacobs, C.; Dubois, Ph.; Jerome, R.; Teyssie, Ph. *Macromolecules* **1991**, *24*, 3027–3034.
(44) Penczek, S.; Duda, A. *Macromol. Symp.* **1996**, *107*, 1–15.
(45) Witzke, D. R.; Kolstad, J. J.; Narayan, R. *Macromolecules* **1997**, *30*, 7075–7085.
(46) Fetters, L. J.; Lohse, D. J.; Richter, D.; Witten, T. A.; Zirkel, A. *Macromolecules* **1994**, *27*, 4639–4647.
(47) Jacobs, M. In *Physical Properties of Polymers Handbook*; AIP Press: New York, 1996.
(48) Schneider, W. A.; Müller, M. F. *J. Mol. Catal.* **1988**, *46*, 395–403.
(49) Müller, A. J.; Arnal, M. L. *Prog. Polym. Sci.* **2005**, *30*, 559–603.
(50) Müller, A. J.; Balsamo, V.; Arnal, M. L. *Adv. Polym. Sci.* **2005**, *190*, 1–63.
(51) Hamley, I. W. In *The Physics of Block Copolymers*; Oxford University Press: New York, 1998.
(52) Bates, F. S.; Fredrickson, G. H. *Phys. Today* **1999**, *52*, 32–38.
(53) Abetz, V.; Simon, P. F. W. *Adv. Polym. Sci.* **2005**, *189*, 125–212.
(54) Leibler, L. *Macromolecules* **1980**, *13*, 1602–1617.
(55) Bates, F. S.; Fredrickson, G. H. *Annu. Rev. Phys. Chem.* **1990**, *41*, 525–547.
(56) Matsen, M. W.; Bates, F. S. *Macromolecules* **1996**, *29*, 1091–1098.
(57) Matsen, M. W.; Thompson, R. B. *J. Chem. Phys.* **1999**, *111*, 7139–7146.
(58) Matsen, M. W.; Bates, F. S. *J. Chem. Phys.* **1997**, *106*, 2436–2448.
(59) (a) Helfand, E.; Tagami, Y. *J. Chem. Phys.* **1972**, *56*, 3592–3601. (b) Helfand, E. *Macromolecules* **1975**, *8*, 552–556. (c) Helfand, E.; Wasserman, Z. R. *Macromolecules* **1976**, *9*, 879–888.
(60) Matsen, M. W. *Phys. Rev. Lett.* **2007**, *99*, 148304/1–148304/4.
(61) (a) Drzal, P. L.; Barned, J. D.; Kofinas, P. *Polymer* **2001**, *42*, 5633–5642. (b) Zalusky, A. S.; Olayo-Valles, R.; Wolf, J. H.; Hillmyer, M. A. *J. Am. Chem. Soc.* **2002**, *124*, 12761–12773.
(62) Mori, Y.; Lim, L. S.; Bates, F. S. *Macromolecules* **2003**, *36*, 9879–9888.
(63) Phatak, A.; Lim, L. S.; Reaves, C. K.; Bates, F. S. *Macromolecules* **2006**, *39*, 6221–6228.
(64) Semba, T.; Kitagawa, K.; Ishiaku, U. S.; Hamada, H. *J. Appl. Polym. Sci.* **2006**, *101*, 1821–1825.
(65) Perego, G.; Cella, G. D.; Bastioli, C. *J. Appl. Polym. Sci.* **1996**, *59*, 37–43.
(66) Bigg, D. M. *Adv. Polym. Technol.* **2005**, *24*, 69–82.
(67) Values are based on at least six measurements per sample.
(68) Of notable exception is sample LCL (35−16−35), having an average ε_b value of 180%, with an uncertainty of equal magnitude. This feature stems from three of the measurements having strain beyond 600%, while the remaining samples behaved similarly to the representative examples shown in Figure 8 with elongations between 30 and 50%.

MA900368A